Am J Transl Res 2021;13(9):10288-10297
www.ajtr.org /ISSN:1943-8141/AJTR0133120

Original Article

The feasibility of modified pancreatogastrostomy *in vivo* and its effect on intestinal microecology

Guoliang Shen[1], Luning Wu[2], Hangdong Jia[3], Junwei Liu[1]

[1]*General Surgery, Department of Hepatobiliary and Pancreatic Surgery and Minimal Invasive Surgery, Zhejiang Provincial People's Hospital, Affiliated People's Hospital, Hangzhou Medical College, Hangzhou 310014, Zhejiang, China;* [2]*Thyroid Gland Breast Surgery, Dongyang People's Hospital, Jinhua 322100, Zhejiang, China;* [3]*Hepatobiliary Pancreatic Surgery, Zhejiang Chinese Medical University, Hangzhou 310000, Zhejiang, China*

Received March 14, 2021; Accepted July 7, 2021; Epub September 15, 2021; Published September 30, 2021

Abstract: Purpose: To evaluate the feasibility of modified binding pancreatogastrostomy (MBPA) by comparing it with traditional pancreatogastrostomy (TPA) and to determine the surgical effects on the intestinal microecology. Methods: The surgical effects on the intestinal microecology of female Bama minipigs (n = 20) were determined by measuring the expressions of the intestinal microbial proteins in the gastric juice, gastric mucosa, and feces before and after MBPA and TPA. We then constructed an integrated interaction network based on the metabolomics and 16S amplicon data, the microbiota, the metabolites, and the associated pathways. Results: The average time required for anastomosis was significantly lower after MBPA than after TPA, but the breaking force did not significantly differ between them. We identified 25 and 51 differentially expressed metabolites and microbiota, respectively. An interaction network was constructed using 16 metabolites (including pyruvic and lactic acids), 27 microbiota (including *Ruminococcaceae*_UCG-00) and six pathways (including pyruvate metabolism). Conclusion: Anastomosis might be achieved sooner and with less pancreatic leakage using MBPA compared with TPA. Pancreatogastrostomy inhibits *Ruminococcaceae* activity, leading to increased expressions of pyruvic and lactic acids in the gut.

Keywords: Traditional pancreatogastrostomy, modified binding pancreatogastrostomy, intestinal microecology, differential microbiota, differential metabolites, metabolic pathways

Introduction

A pancreatic fistula (PF) is a serious complication that follows acute and chronic pancreatitis and abdominal surgery, especially pancreatic and trauma surgery [1]. A traditional pancreatogastrostomy (TPA) is considered clinically safe, and it can prevent PF occurrence [2]. It is conducted to anastomose the pancreatic stump with the posterior wall of the stomach during a pylorus-preserving pancreatoduodenectomy [3]. However, TPA is complicated, and anastomosis takes a long time [4]. Therefore, traditional surgical methods need to be upgraded to improve the clinical effectiveness and feasibility of TPA [5].

Novel surgical techniques, such as anastomosis based on a laparoscopic intracorporeal pancreaticogastrostomy, are breakthroughs that improve TPA in clinical practice [5]. Laparoscopic central pancreatectomy combined with pancreaticogastrostomy might be feasible [6]. These modified anastomotic procedures are safer and more reliable and lower the rate of postoperative PFs [7]. However, all surgical procedures inevitably involve a breach in the epithelial barrier that is colonized by microorganisms, and the influences of different surgical approaches vary on the microbiota [8]. Under normal conditions, the intestinal microbiota provides resistance to pathogens [9]. Major intestinal reconstruction alters the intestinal microbiota, which might contribute to some of the benefits of these procedures, but it might also contribute to postsurgical complications [10]. In other words, evaluating new surgical procedures depends not only on their convenience and direct effects, but also on their influence on the intestinal flora. Thus, a molecular and functional understanding of the responses of the gastrointestinal tract to alterations in its

microbiota are necessary for improving surgical safety and further reducing complications [11].

Therefore, we developed a modified binding pancreatogastrostomy (MBPA) in experimental animal models and then compared its surgical effects with those of TPA. The effects of pancreatogastrostomy on the intestinal microecology were analyzed by measuring the expression of the intestinal microecological proteins in the gastric juice, gastric mucosa, and feces before and after surgery. We aimed to determine the clinical feasibility and effects of MBPA, as well as the influence of pancreatogastrostomy on intestinal microecology.

Materials and methods

Animal information

Twenty female Bama minipigs (*Sus scrofa domestica*; average weight: 30.65 kg; License No. scxk (Su) 2011-0002; Taizhou Taihe Biotechnology Co., Ltd., Beijing, China) were fed a standard diet and housed in a standard environment. The local ethics committee approved the study, and all the experiments proceeded according to the *Guide for the Care and Use of Laboratory Animals* established by Zhejiang University of Traditional Chinese Medicine (Approval No: ZSLL-2015-88).

Experimental design

We flipped a coin to randomly assign the pigs to groups that underwent anastomosis using TPA or MBPA. The pigs were fasted for 1 day, then they were all anesthetized using an intravenous injection of diazepam (0.2 mg/kg) + fentanyl (10 μg/kg) + ketamine (2 mg/kg) + scoline (3 mg/kg), and their pancreases were exposed. We severed a large pancreatic lobe near the duodenum. The proximal part was ligated, and the distal pancreatic duct was inserted into a pancreatic duct support tube (Terumo Corp., Tokyo, Japan) and anastomosed to the adjacent gastric wall at the incision site. Specifically, a similarly sized opening was made on the side of the great curvature of the stomachs of the TPA group using 3-0 (or 4-0) Prolene sutures (Johnson & Johnson, New Brunswick, NJ, USA). The pancreatic stump was then placed in the gastric cavity. The entire gastric wall layer and the pancreatic parenchyma were continuously sutured with Prolene from the posterior to the anterior wall of the anastomotic stoma. A support tube was placed in the pancreatic duct, and three stitches of the gastric serosa and pancreatic parenchyma were intermittently strengthened after one circle of suturing. We used 3-0 Prolene to suture an embedding line at the incision of the great curvature of the stomach in the MBPA group. We then placed the broken end of the pancreas in the gastric cavity and the pancreatic duct support tube in the pancreatic duct, fixed the position of the anastomosis, and tightened the embedding line to fix the pancreas and complete the pancreatogastric anastomosis. Thereafter, a drainage tube was placed under the anastomosis. All the pigs were fasted for 2 days without antibiotics, and the same surgeon performed all the procedures.

Identification of the experimental indicators

We detected the postoperative pancreatic leakage by collecting blood samples from the posterior ear veins of all the pigs before the anesthesia. The baseline serum amylase values were measured in the drainage fluid on postoperative days (POD) 3, 5, and 7. Postoperative pancreatic leakage was considered when the serum amylase content was 3-fold the base value in the drainage fluid. Moreover, the time required to achieve total anastomosis was considered to be from the incision of the gastric wall to complete anastomosis. We tested the mechanical anastomotic stoma in all the pigs, which were sacrificed 2 weeks after the surgical procedure. Large tissues of the anastomotic opening were cut and fixed on the pancreatic side. The gastric wall was pulled using a tensiometer. Finally, the amount of force required to disconnect the anastomotic opening was determined, by tensiometry, to be the breaking force.

Specimen collection

Among the nine pig that received MBPA, one pig with postoperative abdominal abscess and two pigs with absence of preoperative fecal samples were excluded from the subsequent omics analysis. The microbiota data were analyzed in the pre-(class 1) and post-(class 2) operative MBPA fecal samples (n = 12 samples per class) collected from the 6 pig intestines. The fecal samples (0.2 ± 0.02 g) were quickly collected into fecal cups without pollution into an ice box, and then immediately placed in sterile Eppendorf tubes with sterile cotton swabs, and stored at -80°C. The stomach fluid samples (classes 1 and 2, n = 12 samples per class) were extracted from the drainage tubes using a sterile needle tube.

Metabolic enrichment analysis

The annotations of these metabolites were matched to their *Kyoto Encyclopedia of Genes and Genome* (KEGG) identities using the MetaboAnalyst database [12]. The KEGG pathways that were significantly enriched in the different metabolites were explored using MBROLE software (version: 2.0) [13] at $P < 0.05$. The enrichment was visualized using R software.

Analysis of the differential microbiota based on the 16s data

The original operational taxonomic unit (OTU) data were normalized using the trimmed mean of M values (TMM) method of the edgeR [14] package in R, followed by a differential analysis. The original OTU table was extracted according to the door and genus information, and the OTUs that were not annotated to the phylum/genus or that were unclassified were deleted. After extraction, the OTUs with the same door/genus were summed as the expression abundance of the door/genus, and the differential microbiota at the phylum/genus levels were obtained.

Interactions among the differential microbiota

Based on the relative abundance of the genera, a correlation coefficient matrix of the genus level was calculated using igraph (version: 1.2.2) and psych (version: 1.8.4) in R. Finally, based on the interaction model of co-occurrence or the co-exclusion of microbes in the microbiota, any possible cooperation or competition between the different microbial communities was inferred.

Prediction of the differential metabolic functions

We predicted 16S functions by automatically annotating the OTU abundance table and the original 16S representative sequence using PICRUSt2 [15]. We then further predicted the community function according to the compositions of the abundant species. We evaluated the significance of the abundance difference pathways based on the information from the KEGG database and the abundance of the OTUs and identified a significant pathway between the groups.

Analysis of the 16S amplicon and the metabolomic integration

The common functions of the differential OUT and differential metabolites were considered to be co-pathways that were affected by the intestinal flora and associated with the disease. We analyzed the significantly correlated differential flora at the genus level and the metabolites, and an association network of the flora and the differential metabolites was constructed using Cytoscape software.

Statistical analysis

Significantly different metabolites and the related information between classes 1 and 2 were obtained based on the orthogonal projections to the latent structures using discriminant analysis (OPLS-DA) and t-tests. The variable importance in the projection (VIP) of OPLS-DA > 1 and $P < 0.1$ (t-test) were established as cut-off values for metabolite investigations. The differential analysis of OTU and the differential metabolic functions were analyzed using the quasi-likelihood (QL) F-test method of edgeR, and the adjusted $P < 0.05$ was considered the cut-off value. The correlations among the differential microbiota and the correlations among the differential flora and metabolites were calculated using Pearson correlation analyses. $P < 0.05$ and $|r| > 0.8$ were used as cut-off values to screen the significantly correlated microbial communities, and the significantly correlated differential flora and the metabolites.

Results

Comparison of the experimental indicators between TPA and MBPA

Nine and 11 pigs underwent MBPA and TPA, respectively. The pancreatic duct could not be accessed in one pig in each group. The average time required for anastomosis was significantly shorter in the MBPA than in the TPA group (8.44 ± 3.54 vs. 17.00 ± 6.42 min; $P < 0.01$). However, an intraperitoneal abscess was found during autopsy in one pig from the MBPA group at 2 weeks after the surgery, and one pig in the TPA group died on POD 3. The breaking force did not significantly differ between the MBPA and TPA groups (17.24 ± 5.64 vs. 18.56 ± 7.00 cattle, $P = 0.659$; Supplementary Table 1). Furthermore, the incidence of postoperative

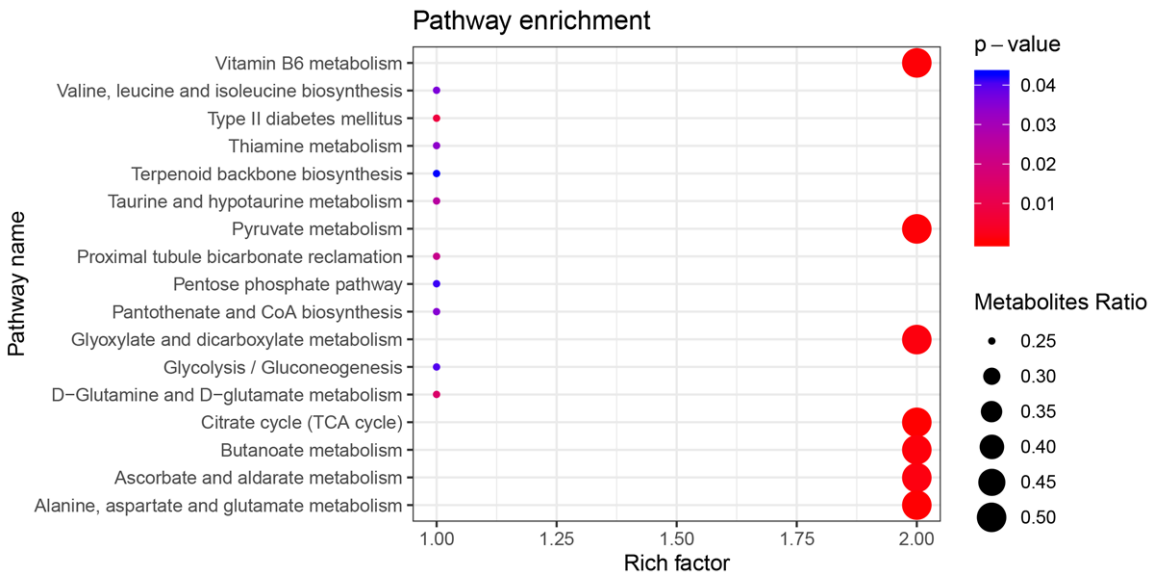

Figure 1. Differential metabolite-enriched KEGG pathways. X-axis, number of metabolites (rich factor); Y-axis, name of each pathway. Circles, ratio of metabolites enriched in the pathway. Larger nodes indicate higher metabolite ratios. Smaller *p* values indicate more statistical significance.

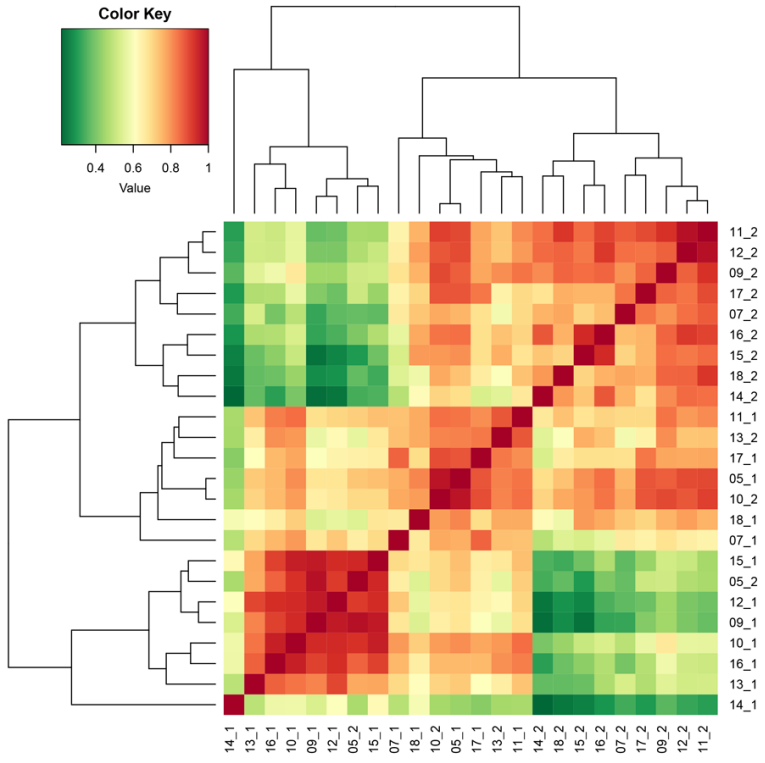

Figure 2. Correlation heatmap of the differential microbiota at the genus level. Red, blue, and yellow blocks, respectively, represent microbiota that are upregulated, downregulated, and not significantly different.

pancreatic leakage was significantly higher in the TPA (n = 4 [36.36%]) than in the MBPA group (n = 0 [0%]) P = 0.003; Supplementary Table 2).

Differential metabolites and the associated pathway analysis

We investigated 25 differential metabolites among the samples from the two groups. The findings of the KEGG pathway enrichment analyses showed that these differential metabolites were mainly enriched in 17 pathways ($P < 0.05$) and included vitamin B6, pyruvate, and butanoate metabolism (**Figure 1**).

Differential microbiota investigation

Among the 112 differentially expressed OTUs, 59 and 53 were up- and downregulated, respectively. Moreover, among the 51 differential microbiota, 18 and 33 were up- and downregulated, respectively, at the genus level. **Figure 2** shows a correlation heatmap of the differential microbiota at the genus level.

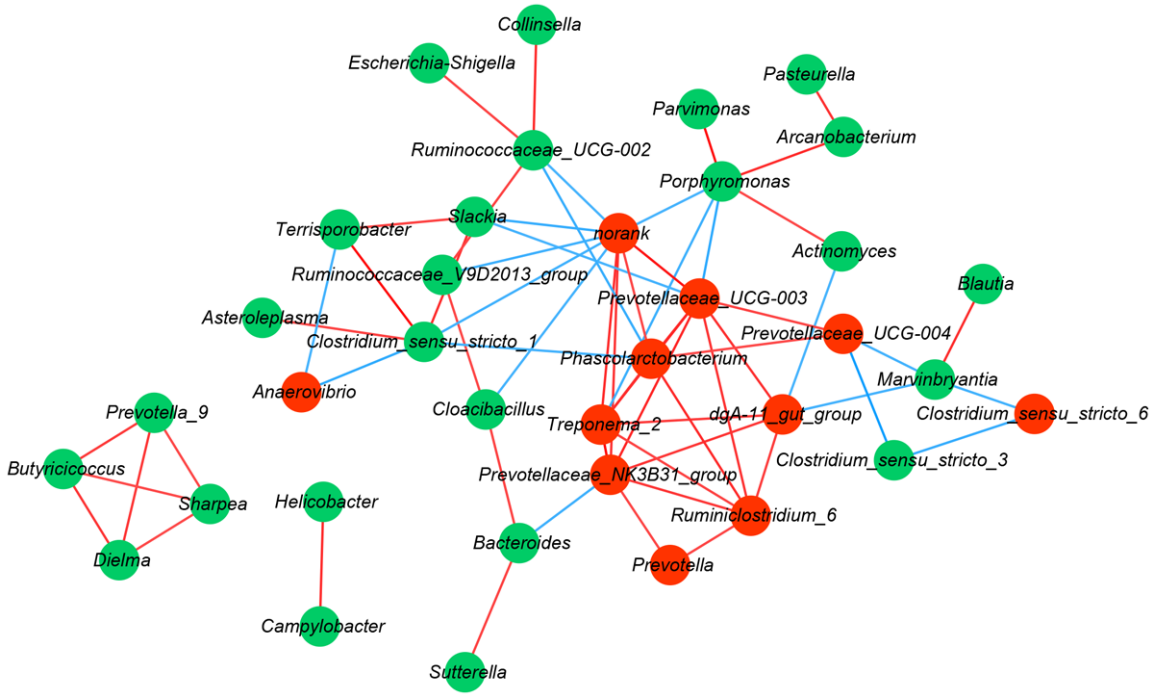

Figure 3. An interaction network constructed based on the upregulated and downregulated differential microbiota at the genus level. The red and green circles indicate upregulated and downregulated differential microbiota, respectively. The red and blue lines between the two nodes indicate positive and negative interactions among the microbiota, respectively.

Interaction network and pathway analysis of the differential microbiota

We constructed an interaction network from the findings of the differential microbiota at the genus level. The results revealed 36 nodes and 63 interactions in the network (**Figure 3**). An investigation of the metabolic pathways using Picrust2 uncovered 52 pathways, including folate biosynthesis, a two-component system, and bacterial chemotaxis, which were enriched by differential microbiota (**Figure 4**).

Investigation of the amplicon and metabolome integration

The results of the VENN plots of the 52 and 17 differential pathways in the 16S amplicon and metabolome analyses revealed six co-pathways, including the citrate cycle (TCA cycle), valine-leucine and isoleucine biosynthesis, pyruvate, glyoxylate and dicarboxylate metabolism, butanoate metabolism, and vitamin B6 metabolism (Supplementary Figure 1). Based on the results of the amplicon and metabolome analyses, our integration network consisted of 16 metabolites (including pyruvic acid, lactic acid, and alpha-ketoglutaric acid), 27 differential microbiotas at the genus level (*Treponema*_2, *Prevotellaceae*_NK3B31_group, *Prevotella*, *Collinsella*, *Ruminococcaceae*_V9D2013_group, and *Ruminococcaceae*_UCG-002), and 60 interactions (**Figure 5**). **Figure 6** shows interactions among the differential microbiota and metabolites, and the associated pathways. The results revealed several microbiota-metabolite-pathway interactions, such as the *Ruminococcaceae*-lactic acid-pyruvate metabolism and the *Ruminococcaceae*-pyruvic acid-pyruvate metabolism.

Discussion

Although TPA is the classical surgical technique for treating PF, its complex process and its long anastomosis duration hinder its routine clinical use. Here, we introduced a modified procedure (MBPA) in animal models and compared the clinical effects and postoperative enteral microbiota with those of TPA. The results showed a significantly shorter average elapsed time to anastomosis in the MBPA than in the

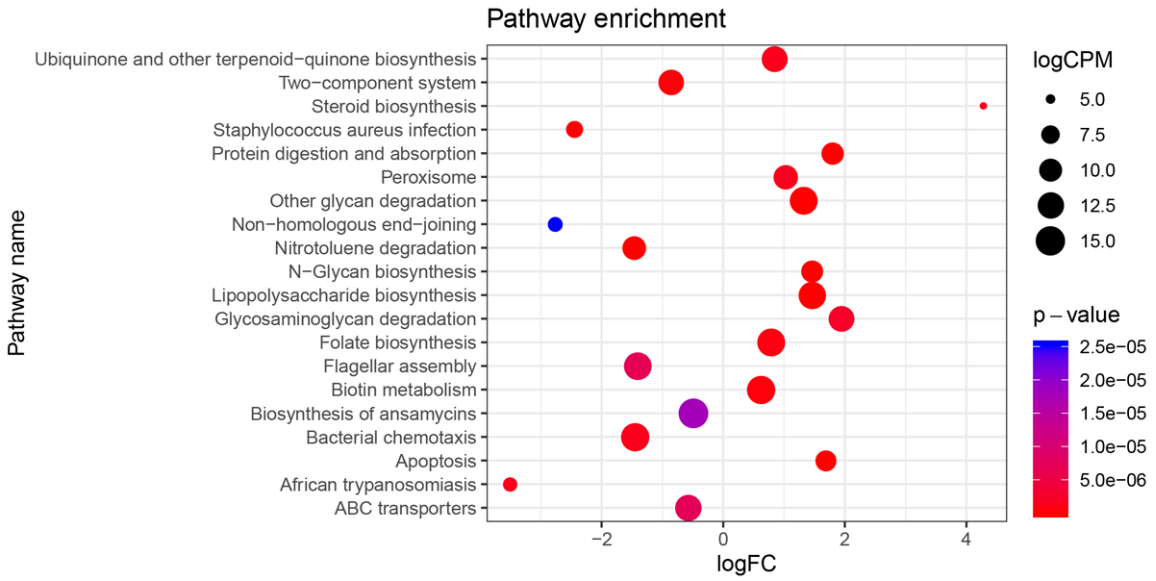

Figure 4. The findings of the differential microbiota enriched KEGG pathway analysis. X-axis, logFC; Y-axis, pathways. The circles represent the ratios of the metabolites enriched in the pathways. Larger nodes represent higher metabolite ratios. Smaller *p* values represent more statistically significant results.

TPA group, and the breaking force did not significantly differ between them. Moreover, 25 differential metabolites and 51 differential microbiota at the genus level were revealed in the samples before and after the pancreatogastrostomies. We then constructed an interaction network using 16 metabolites (including pyruvic and lactic acids), 27 differential microbiota at the genus level (including Ruminococcaceae_UCG-00), and six pathways (including pyruvic metabolism).

Pancreatic anastomotic leakage is a persistent problem after a pancreaticoduodenectomy, especially when the pancreas is soft and nonfibrotic [16]. Although TPA can prevent the occurrence of PFs [17] and has been shown to be safe and effective, most anastomotic methods require many sutures or complicated operations [18]. One modified pancreatogastrostomy technique that combines one binding purse-string and two transfixing mattress sutures between the pancreatic stump and the posterior gastric wall showed that all the fistulas were resolved without further intervention [19]. However, the advent of laparoscopy and other technologies has led to the gradual replacement of traditional surgical methods by minimally- or non-invasive surgeries [20]. A laparoscopic, one-anastomosis gastric bypass is clinically safer and more effective than the classic method because the procedure is simpler and shorter [21]. Therefore, simplifying the surgery and decreasing the incidence of pancreatic leakage are targets for adapting TPA to more modern procedures such as laparoscopy. Here, we simplified the process of TPA by embedding a purse line layer in the gastric wall and tightening the purse line after the pancreatic stump was included. The results showed a significantly shorter average duration to achieve anastomosis in the MBPA than in the TPA group, and that breaking force did not significantly differ between the two groups. Thus, we found that MBPA significantly shortened the amount of time needed for anastomosis, reduced the incidence of pancreatic leakage, and simplified the procedure, thus providing information about its application in laparoscopic surgery.

Human gastrointestinal tract microbiota contains various complex populations of many bacterial species, along with a few fungi, protozoa, and archaea [22]. The intestinal microbiota environment significantly varies after surgery [23]. The intestinal “microbiome” shifts to a “pathobiome” that governs the course and outcome of sepsis after a surgical injury [24]. *Ruminococcaceae* is a family of bacteria in the class Clostridia, which inhabits the human gut [25]. It is the most abundant bacterial family in the mammalian gut and is associated with the

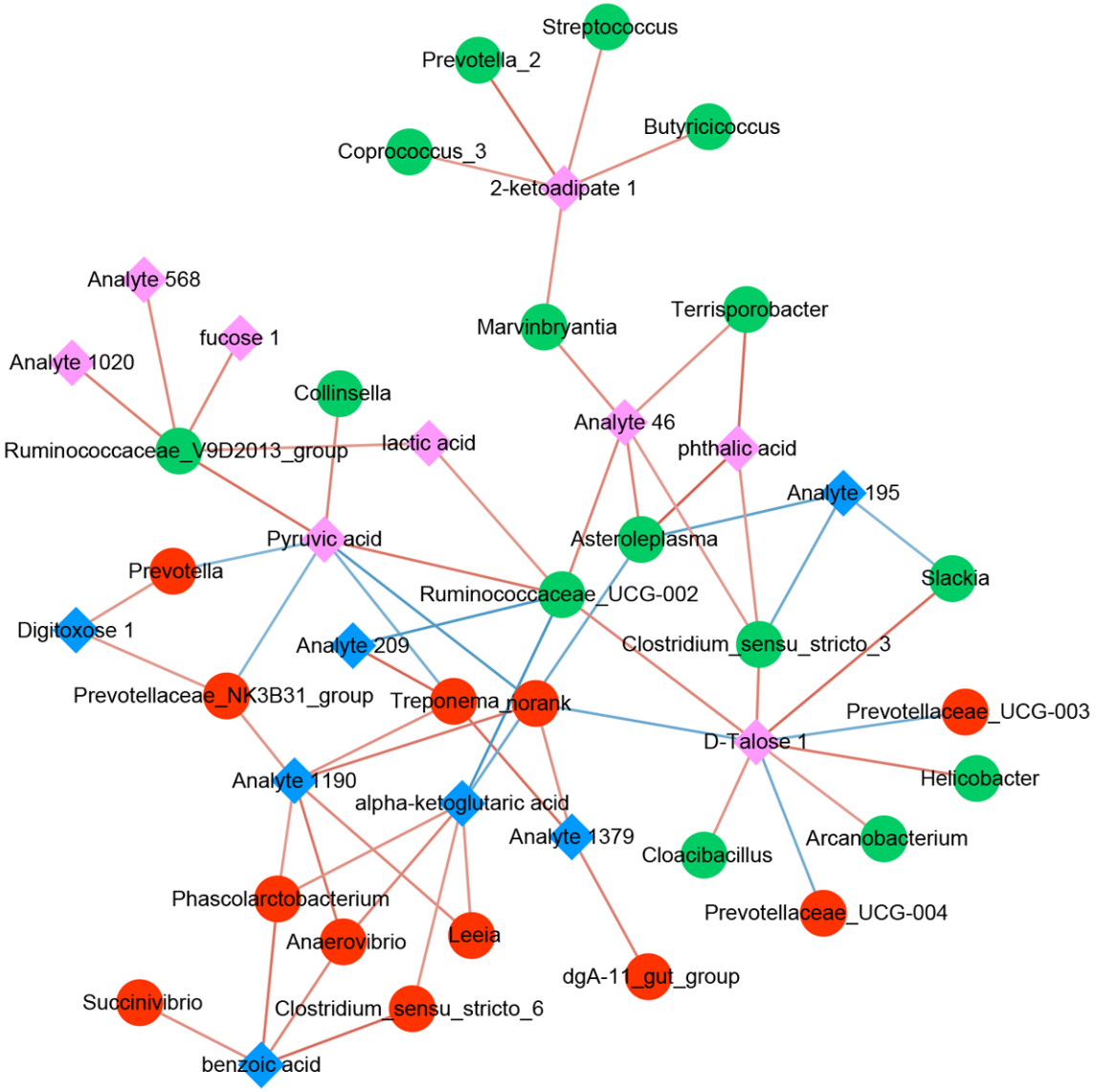

Figure 5. An integrated interaction network comprising differential microbiota and differential metabolites. The red and green circles indicate upregulated and downregulated microbiota, respectively. The blue and pink diamonds represent downregulated and upregulated metabolites, respectively. The red and blue lines between the nodes indicate the positive and negative relationships, respectively.

maintenance of gut health [26]. A pyrosequencing study of an animal model revealed *Ruminococcaceae* microbial communities all along the gastrointestinal tract [27]. Lactic and pyruvic acids are two common metabolites involved in the normal metabolism of *Ruminococcaceae* [25, 28]. High concentrations of postoperative and intraoperative lactic acid are associated with prognosis after surgery [29]. The serum pyruvic acid expression levels can serve as markers for cancer detection [30]. Here, low levels of *Ruminococcaceae* were expressed in pig microbiota before and after pancreatogastrostomies. Our correlation analysis of the differential microbiota, the differential metabolites, and the associated pathways showed that *Ruminococcaceae*-lactic acid-pyruvate metabolism and *Ruminococcaceae*-pyruvic acid-pyruvate metabolism were microbiota-metabolite-pathway interactions in our network. Thus, we speculated that pancreatogastrostomy might inhibit the activity of *Ruminococcaceae* and lead to a high abundance of pyruvic and lactic acids in the pyruvic acid metabolism pathway.

Mammals have a diverse and very active microbial community that closely correlates with dis-

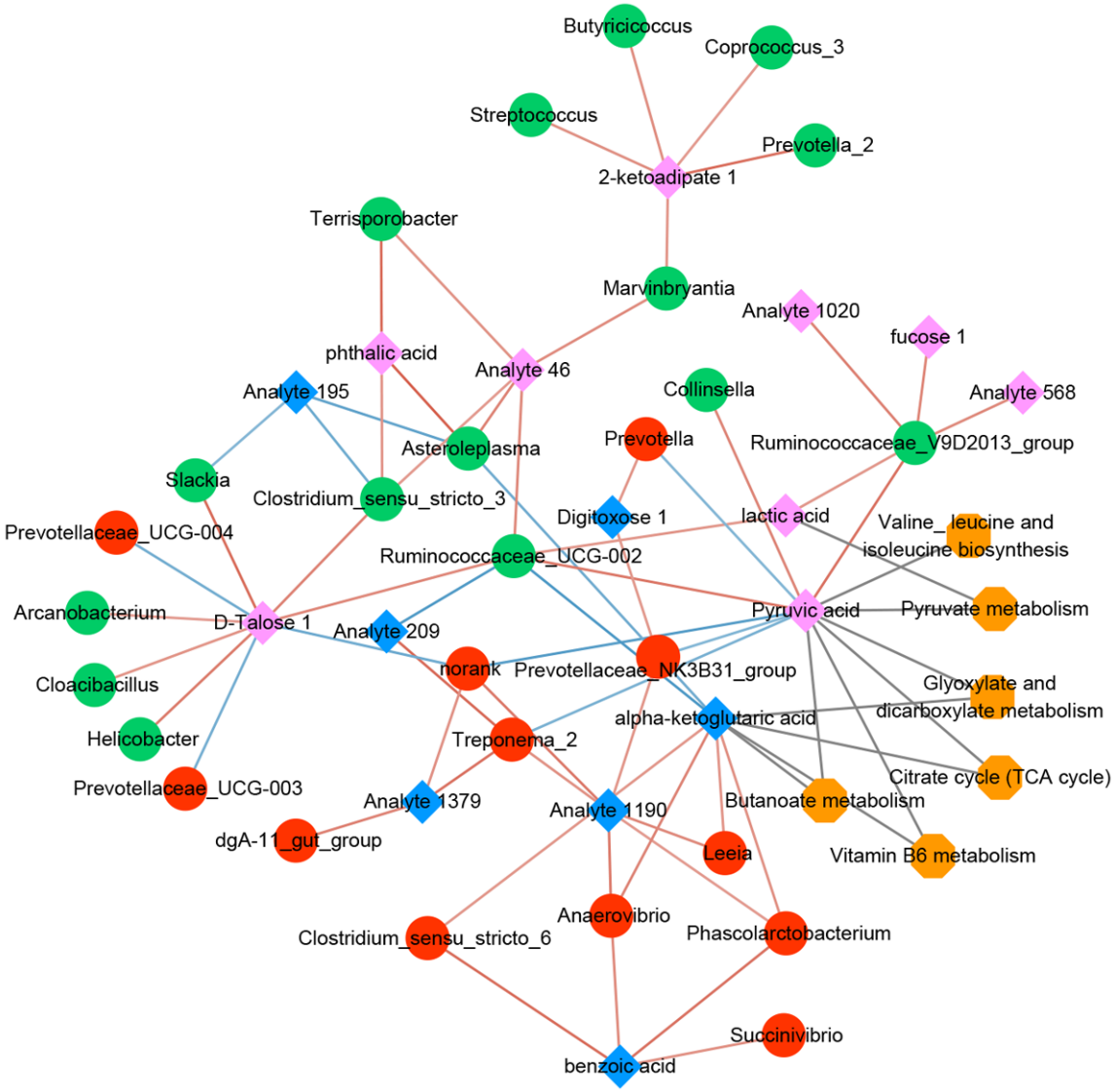

Figure 6. The interaction relationships among the differential microbiota, the differential metabolites, and the associated pathways. The red and green circles indicate upregulated and downregulated microbiota, respectively. The blue and pink diamonds represent the downregulated and upregulated metabolites, respectively. The red and blue lines between two nodes indicate the positive and negative relationships, respectively. The orange hexagon indicates the metabolic pathway.

ease when imbalanced [31]. For example, microbial communities and their metabolites are not only required for immune homeostasis, they also affect the host's susceptibility to various diseases [32]. Crosstalk between the microbial community and the host partly depends on the metabolite secretions. Metabolites in the host serve as signaling molecules and substrates for metabolic reactions; this provides a snapshot in times of extremely complicated host physiology [31, 32]. We established a network to investigate the interactions among the differential microbiota and the differential metabolites and found six pathways in common. We speculate that these differential microbial and metabolites influence the post-surgical outcomes by regulating these pathways. However, our results require further verification. The gut microbiota plays an important role in modulating the host response to surgery, immunotherapy, and other interventions. Ecological changes (for instance, immune response fluctuation) can trigger structural and functional alterations of the local microbial community. Such alterations might in turn change the crosstalk between the resident

microbiota and the host from symbiosis to dysbiosis [33]. Since gastrointestinal surgery inevitably involves a breach of the epithelial barrier that is colonized by microbes, preoperative intestinal disinfection is carried out to decrease the likelihood of complications caused by infections. However, the present methods of intestinal disinfection vary considerably among institutions and countries, and little is known about the mechanism of action, the impact on the intestinal flora, or the overall effectiveness of the disinfectants [34]. Therefore, possible mechanisms through which MBPA can induce changes in the microbiota and the metabolites should be investigated in the future. The feasibility and effects of MBPA and its influence on the microbial community and the metabolites were evaluated in animal models. However, the clinical applications should be further confirmed using clinical samples.

In conclusion, MBPA significantly shortens the time to the completion of anastomosis, reduces the incidence of pancreatic leakage, and simplifies the procedure, thus providing information about its use in laparoscopic surgery. Moreover, pancreatogastrostomies might inhibit the activity of *Ruminococcaceae*, leading to high expressions of pyruvic and lactic acids in the pyruvic acid metabolism pathway.

Acknowledgements

This work was supported by the Zhejiang Province Foundation [grant number Y2015-34516]. The funder had no role in the study design, the data collection and analysis, the decision to publish, or the preparation of the manuscript.

Disclosure of conflict of interest

None.

Address correspondence to: Junwei Liu, General Surgery, Department of Hepatobiliary and Pancreatic Surgery and Minimal Invasive Surgery, Zhejiang Provincial People's Hospital, Affiliated People's Hospital, Hangzhou Medical College, Shangtang Road 158#, Hangzhou 310014, Zhejiang, China. Tel: +86-0571-85893395; Fax: +86-0571-85335-800; E-mail: Liujunwei@hmc.edu.cn

References

[1] Williamsson C, Ansari D, Andersson R and Tingstedt B. Postoperative pancreatic fistula-impact on outcome, hospital cost and effects of centralization. HPB (Oxford) 2017; 19: 436-442.

[2] Shrikhande SV, Sivasanker M, Vollmer CM, Friess H, Besselink MG, Fingerhut A, Yeo CJ, Fernandez-delCastillo C, Dervenis C, Halloran C , Gouma DJ, Radenkovic D, Asbun HJ, Neoptolemos JP, Izbicki JR, Lillemoe KD, Conlon KC, Fernandez-Cruz L, Montorsi M, Bockhorn M, Adham M, Charnley R, Carter R, Hackert T, Hartwig W, Miao Y, Sarr M, Bassi C and Büchler MW; International Study Group of Pancreatic Surgery (ISGPS). Pancreatic anastomosis after pancreatoduodenectomy: a position statement by the international study group of pancreatic surgery (ISGPS). Surgery 2017; 161: 1221-1234.

[3] Quesada R, Simón C, Radosevic A, Poves I, Grande L and Burdío F. Morphological changes of the pancreas after pancreaticoduodenectomy. Sci Rep 2019; 9: 14517.

[4] Straja N, Daha C, Bratucu E, Cirimbei C, Prunoiu V, Alecu M, Ionescu S, Mareæ T and Simion L. Pancreaticojejunostomy-risk anastomosis after cephalic pancreaticoduodenectomy. Chirurgia (Bucur) 2015; 110: 339-345.

[5] Puntambekar SP, Mehta MJ, Manchekar MM, Chitale M, Panse M, Jathar A and Umalkar R. Laparoscopic intracorporeal pancreaticogastrostomy in total laparoscopic pancreaticoduodenectomy-a novel anastomotic technique. Indian J Surg Oncol 2019; 10: 274-279.

[6] Hong D, Xin Y, Cai X and Peng S. Application of binding pancreatogastrostomy in laparoscopic central pancreatectomy. World J Surg Oncol 2012; 10: 223.

[7] Osman MM and Abd El Maksoud W. Evaluation of a new modification of pancreaticogastrostomy after pancreaticoduodenectomy: anastomosis of the pancreatic duct to the gastric mucosa with invagination of the pancreatic remnant end into the posterior gastric wall for patients with cancer head of pancreas and periampullary carcinoma in terms of postoperative pancreatic fistula formation. Int J Surg Oncol 2014; 2014: 490386.

[8] Aron-Wisnewsky J, Doré J and Clement K. The importance of the gut microbiota after bariatric surgery. Nat Rev Gastroenterol Hepatol 2012; 9: 590-8.

[9] Alverdy J, Hyoju S, Weigerinck M and Gilbert J. The gut microbiome and the mechanism of surgical infection. Br J Surg 2017; 104: e14-e23.

[10] Guyton K and Alverdy JC. The gut microbiota and gastrointestinal surgery. Nat Rev Gastroenterol Hepatol 2017; 14: 43-54.

[11] Tseng CH, Lin JT, Ho HJ, Lai ZL, Wang CB, Tang SL and Wu CY. Gastric microbiota and predicted gene functions are altered after subtotal

gastrectomy in patients with gastric cancer. Sci Rep 2016; 6: 20701.
[12] Chong J, Soufan O, Li C, Caraus I, Li S, Bourque G, Wishart DS and Xia J. MetaboAnalyst 4.0: towards more transparent and integrative metabolomics analysis. Nucleic Acids Res 2018; 46: W486-W494.
[13] Lopez-Ibanez J, Pazos F and Chagoyen M. MBROLE 2.0-functional enrichment of chemical compounds. Nucleic Acids Res 2016; 44: W201-4.
[14] Robinson MD, McCarthy DJ and Smyth GK. edgeR: a bioconductor package for differential expression analysis of digital gene expression data. Bioinformatics 2010; 26: 139-140.
[15] Douglas GM, Maffei VJ, Zaneveld JR, Yurgel SN, Brown JR, Taylor CM, Huttenhower C and Langille MGI. PICRUSt2 for prediction of metagenome functions. Nat Biotechnol 2020; 38: 685-688.
[16] Reid-Lombardo KM, Farnell MB, Crippa S, Barnett M, Maupin G, Bassi C and Traverso LW; Pancreatic Anastomotic Leak Study Group. Pancreatic anastomotic leakage after pancreaticoduodenectomy in 1,507 patients: a report from the pancreatic anastomotic leak study group. J Gastrointest Surg 2007; 11: 1451-8; discussion 1459.
[17] Ikon H, Morimura R, Arita T, Kosuga T, Konishi T, Murayama Y, Komatsu S, Shiozaki A, Kuriu Y and Nakanishi M. The experience of 133 pancreatoduodenectomy with pancreaticogastric anastomosis. Pancreatology 2016; 16: S150-S151.
[18] Fujii T, Sugimoto H, Yamada S, Kanda M, Suenaga M, Takami H, Hattori M, Inokawa Y, Nomoto S, Fujiwara M and Kodera Y. Modified Blumgart anastomosis for pancreaticojejunostomy: technical improvement in matched historical control study. J Gastrointest Surg 2014; 18: 1108-1115.
[19] Bartsch D, Langer P, Kanngiesser V, Fendrich V and Dietzel K. A simple and safe anastomosis for pancreatogastrostomy using one binding purse-string and two transfixing mattress sutures. Int J Surg Oncol 2012; 2012: 718637.
[20] Matsuda M, Haruta S, Shinohara H, Sasaki K and Watanabe G. Pancreaticogastrostomy in pure laparoscopic pancreaticoduodenectomy-a novel pancreatic-gastric anastomosis technique. BMC Surg 2015; 15: 80.
[21] Carbajo MA, Luque-de-León E, Jiménez JM, Ortiz-de-Solórzano J, Pérez-Miranda M and Castro-Alija MJ. Laparoscopic one-anastomosis gastric bypass: technique, results, and long-term follow-up in 1200 patients. Obes Surg 2017; 27: 1153-1167.
[22] Stanley D, Hughes RJ, Geier MS and Moore RJ. Bacteria within the gastrointestinal tract microbiota correlated with improved growth and feed conversion: challenges presented for the identification of performance enhancing probiotic bacteria. Front Microbiol 2016; 7: 187.
[23] Ohigashi S, Sudo K, Kobayashi D, Takahashi T, Nomoto K and Onodera H. Significant changes in the intestinal environment after surgery in patients with colorectal cancer. J Gastrointest Surg 2013; 17: 1657-1664.
[24] Krezalek MA, DeFazio J, Zaborina O, Zaborin A and Alverdy JC. The shift of an intestinal "microbiome" to a "pathobiome" governs the course and outcome of sepsis following surgical injury. Shock 2016; 45: 475-82.
[25] Rainey FA. Family VIII. Ruminococcaceae fam. nov. Bergey's Manual of Systematic Bacteriology 2009; 3: 1016.
[26] Biddle A, Stewart L, Blanchard J and Leschine S. Untangling the genetic basis of fibrolytic specialization by Lachnospiraceae and Ruminococcaceae in diverse gut communities. Diversity 2013; 5: 627-640.
[27] Wang J, Fan H, Han Y, Zhao J and Zhou Z. Characterization of the microbial communities along the gastrointestinal tract of sheep by 454 pyrosequencing analysis. Asian-Australas J Anim Sci 2017; 30: 100-110.
[28] Zhu X, Zhou Y, Wang Y, Wu T, Li X, Li D and Tao Y. Production of high-concentration n-caproic acid from lactate through fermentation using a newly isolated ruminococcaceae bacterium CPB6. Biotechnol Biofuels 2017; 10: 102.
[29] Connolly C, Stättner S, Niederwieser T and Primavesi F. Systematic review on peri-operative lactate measurements to predict outcomes in patients undergoing liver resection. J Hepatobiliary Pancreat Sci 2020; 27: 359-370.
[30] Bhat MA, Prasad K, Trivedi D, Rajeev B and Battur H. Pyruvic acid levels in serum and saliva: a new course for oral cancer screening? J Oral Maxillofac Pathol 2016; 20: 102-5.
[31] Levy M, Blacher E and Elinav E. Microbiome, metabolites and host immunity. Curr Opin Microbiol 2017; 35: 8-15.
[32] Rooks MG and Garrett WS. Gut microbiota, metabolites and host immunity. Nat Rev Immunol 2016; 16: 341-352.
[33] Villéger R, Lopès A, Carrier G, Veziant J, Billard E, Barnich N, Gagnière J, Vazeille E and Bonnet M. Intestinal microbiota: a novel target to improve anti-tumor treatment? Int J Mol Sci 2019; 20: 4584.
[34] Guyton K and Alverdy JC. The gut microbiota and gastrointestinal surgery. Nat Rev Gastroenterol Hepatol 2017; 14: 43-54.

Supplementary Table 1. The anastomotic time, breaking force and postoperative complication information for the pigs in the TPA and MBPA

Number	Operation method	Anastomosis time	Breaking force	Remarks
1	MBPA	5	18.27	
2	TPA	12		D3 death
3	TPA	8	16.71	
4	TPA	10	22.16	
5	MBPA	9	7.13	
6	MBPA	14	12.38	
7	MBPA	13	19.53	
8	TPA	26	36.62	
9	MBPA	11	21.11	
10	TPA	12	19.17	
11	TPA	27	12.12	
12	MBPA	8	26.05	Abdominal abscess
13	TPA	17	16.38	
14	MBPA	6	20.71	
15	MBPA	5	16.89	
16	MBPA	5	13.1	
17	TPA	14	13.74	
18	TPA	22	18.29	
19	TPA	21	13.41	
20	TPA	18	17.03	

Notes: TPA, traditional pancreaticogastric anastomosis; MBPA, modified binding pancreaticogastric anastomosis; D3, 3 days after the operation.

Supplementary Table 2. The ratios of the amylase and pancreatic leakage in the MBPA and TPA

Number	Preoperative	Postoperative D3	Postoperative D5	Postoperative D7	Pancreatic leakage
1	1497		1269	1348	n
2	799				y
3	875	10254		2046	y
4	418	1280			y
5	2113	3927			n
6	1746	539	1488	152	n
7	3485	2088		349	n
8	2149	1900		1492	n
9	1086	1209	223	125	n
10	1857	2268	451	256	n
11	2001	1500	204		n
12	5480	9260		29	n
13	2685	4065		50	n
14	2036		1473	74	n
15	1556		1547	287	n
16	2218		1576	227	n
17	1445		1990	1421	n
18	1270		3828		y
19	656		392		n
20	974	1619	1034		n

Notes: TPA, traditional pancreaticogastric anastomosis; MBPA, modified binding pancreaticogastric anastomosis; D3, 3 days after the operation; D5, 5 days after the operation; D7, 3 days after the operation; y, postoperative pancreatic leakage; n, non-postoperative pancreatic leakage.

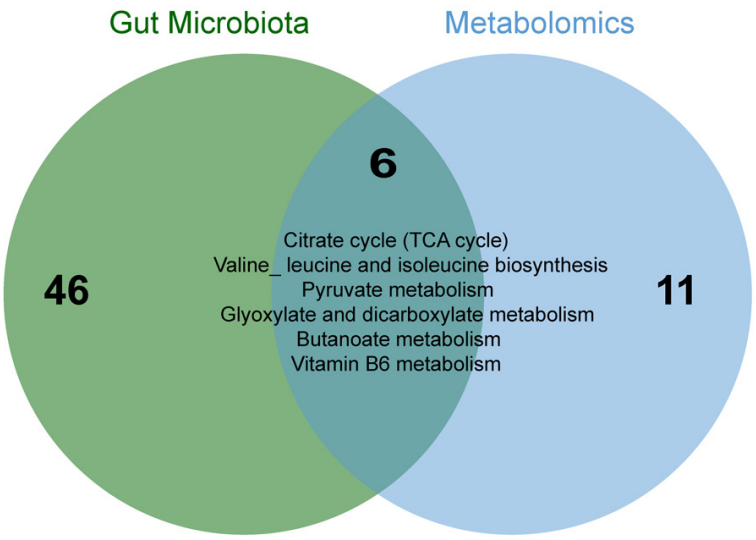

Supplementary Figure 1. The co-pathways between the 52 differential pathways in the 16S amplicons and the 17 differential pathways in metabolome.